THE JOURNAL OF PHYSICAL CHEMISTRY LETTERS
A JOURNAL OF THE AMERICAN CHEMICAL SOCIETY

pubs.acs.org/JPCL

Letter

The DFT-ReaxFF Hybrid Reactive Dynamics Method with Application to the Reductive Decomposition Reaction of the TFSI and DOL Electrolyte at a Lithium−Metal Anode Surface

Yue Liu, Peiping Yu, Yu Wu, Hao Yang, Miao Xie, Liyuan Huai, William A Goddard, III,* and Tao Cheng*

Cite This: *J. Phys. Chem. Lett.* 2021, 12, 1300−1306

Read Online

ACCESS | Metrics & More | Article Recommendations | Supporting Information

ABSTRACT: The high energy density and suitable operating voltage make rechargeable lithium ion batteries (LIBs) promising candidates to replace such conventional energy storage devices as nonrechargeable batteries. However, the large-scale commercialization of LIBs is impeded significantly by the degradation of the electrolyte, which reacts with the highly reactive lithium metal anode. Future improvement of the battery performance requires a knowledge of the reaction mechanism that is responsible for the degradation and formation of the solid-electrolyte interphase (SEI). In this work, we develop a hybrid computational scheme, **Hybrid ab initio molecular dynamics combined with reactive force fields**, denoted **HAIR**, to accelerate Quantum Mechanics-based reaction dynamics (QM-MD or AIMD, for ab initio RD) simulations. The HAIR scheme extends the time scale accessible to AIMD by a factor of 10 times through interspersing reactive force field (ReaxFF) simulations between the AIMD parts. This enables simulations of the initial chemical reactions of SEI formation, which may take 1 ns, far too long for AIMD. We apply the HAIR method to the bis(trifluoromethanesulfonyl)imide (TFSI) electrolyte in 1,3-dioxolane (DOL) solvent at the Li metal electrode, demonstrating that HAIR reproduces the initial reactions of the electrolyte (decomposition of TFSI) previously observed in AIMD simulation while also capturing solvent reactions (DOL) that initiate by ring-opening to form such stable products as CO, CH_2O, and C_2H_4, as observed experimentally. These results demonstrate that the HAIR scheme can significantly increase the time scale for reactive MD simulations while retaining the accuracy of AIMD simulations. This enables a full atomistic description of the formation and evolution of SEI.

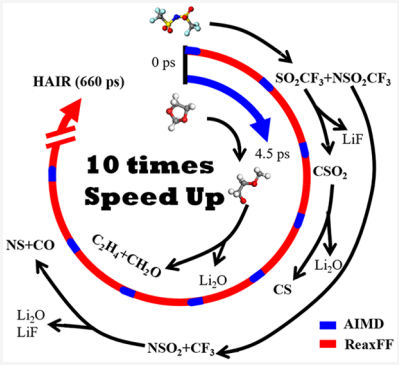

The global population explosion with the concomitant demand for energy and environmental sustainability requires renewable energy technologies based on energy storage with batteries playing an essential part.[1] The high energy density and operating voltage characteristics of rechargeable lithium ion batteries (LIBs) make them most promising candidates to facilitate high energy density storage.[2,3] Typical LIBs combine positive and negative electrodes (the anode and cathode, respectively) with an electrolyte solution containing dissolved lithium salts, which leads to possible reactions and degradation.[4]

Rechargeable lithium ion batteries are widely used for energy storage, but critical obstacles, such as irreversible capacity, safety, and cycle life, have prevented the application of LIBs to such large-scale applications as electric vehicles and aircraft at commercially feasible costs.[5,6] For example, Li metal, which is the most reactive, leads to spontaneous reactions with such electrolytes as bis(trifluoromethanesulfonyl)imide (TFSI). These electrolyte degradation reduction reactions lead to the formation of a solid-electrolyte interphase (SEI) layer that limits the retention of capacity and decreases battery lifecycles.[7,8] To facilitate an optimization toward commercial Li ion battery performance, it is crucial to gain a comprehensive atomistic mechanistic understanding of the SEI formation process and degradation of the electrolyte.[9]

During the charge−discharge cycles of a Li ion battery, SEI films are formed with both inorganic and organic layers, which isolate the electrolyte and electrode by formation of a passivation layer that prevents further reactions.[10] To elucidate the formation and composition of the SEI layer, numerous experimental and theoretical studies have been reported.[11−14] Since the discovery of the passivation layer by Dey[11] in the 1970s, efforts have been made to clarify the nature of SEI from the experiment. In 1985, Nazri[15] identified Li_2CO_3 as a major component of the SEI by combining IR spectroscopy, low-angle X-ray diffraction, and scanning electron microscope (SEM) methods. These experiments identified LiF and Li_2O as major

Received: December 18, 2020
Accepted: January 15, 2021
Published: January 27, 2021

inorganic components, while organic carbonates were identified as major organic components.[16] On the basis of these analyses, Ramos-Sanchez concluded that the composition of the electrolyte and solvent determines the nature of the SEI layer produced.[17,18]

Unfortunately, the components and detailed reaction mechanism of formatting the SEI layer remain far from clear, with experimental resolution of the atomic structure continuing to be a challenge. However, improvements in the atomic-scale simulation are getting to the point where these simulations can provide an effective alternative tool to explore complex reaction processes by tracking the reactive events along the MD trajectories. This provides the means to develop a fundamental understanding of the initial reactions involved in SEI formation and electrolyte degradation.[19] For example, Wang[20] calculated the potential energy surface (PES) of the reaction between Li cation and solvent ethylene carbonate (EC) using density functional theory (DFT) methods. Moreover, a molecular dynamics (MD)-assisted simulation has been widely used to investigate the reduction of electrolyte and SEI formation.[21−23] Camacho-Forero[22] constructed theoretical models of the lithium−metal anode surface with such electrolyte solvents as EC, dimethoxyethane (DME), and dioxolane (DOL). Initial reactions were simulated with ab initio molecular dynamics (AIMD) to describe the Li salts: lithium bis-(trifluoromethanesulfonyl)imide (LiTFSI) or lithium bis-(fluorosulfonyl)imide (LiFSI). They observed that the Li salts in contact with a Li surface react quickly, even before the degradation reduction of solvents.[24−26]

Although AIMD simulations have been demonstrated to be useful in understanding the initial steps of reactions, the computational expense limits the time scale for AIMD simulation to tens of picoseconds (ps), which is not sufficient to explore the SEI film formation process, which may require nanoseconds (ns) or longer. An alternative is to use empirical methods for reactive simulations, such as the reactive force field (ReaxFF), derived to fit quantum-mechanics (QM) calculations and practical up to millions of atoms for nanoseconds and beyond. This can extend the time scale of SEI formation to sufficient time scales to observe the final SEI.[27,28] For example, Bedrov and co-workers[29] developed ReaxFF parameters for singly reduced EC while including Li cations. They investigated the reduction reactions in both the gas phase and solution phase to propose reaction mechanisms.

However, ReaxFF has two problems in simulating batteries. First, sufficiently accurate force-field parameters for battery-related systems may not be available. Thus, ReaxFF parameters are not available for the two most widely used experimental electrolytes: TFSI and FSI (bis(fluorosulfonyl)imide).[23] This explains why few simulations have been reported for these systems, despite their importance. Second, the current framework of ReaxFF does not include explicit consideration of the electron, which may impede describing electrochemical reactions that involve electron (e^-) transfer. Strategies that explicitly include electrons, such as the electron force field (eFF) and eReaxFF[30] or more elaborate treatment of charge,[31] show promising application, but they have not yet been adequate for the above two systems.

In this work, we develop an alternative hybrid scheme: **Hybrid ab initio and reactive force field reactive dynamics (HAIR)**, which combines AIMD and ReaxFF reactive dynamics. The advantage of the HAIR method is that AIMD simulations can describe accurately the localized electrochemical reactions, while the ReaxFF MD can describe the longer-range and longer-time chemical reactions in the electrolyte along with the mass transfer. This HAIR scheme also alleviates the burden of fitting the ReaxFF parameters to describe every local bond-breaking barrier accurately, because this is handled by the AIMD steps.

In this work, we started with the ReaxFF parameters developed by Islam et al.,[32] which we optimized further using training data from our accurate QM calculations that in turn was combined with the Monte Carlo simulated annealing (MC) force field optimization method.[33,34] The final ReaxFF parameters are in the Supporting Information. We then apply HAIR reactive dynamics to simulate the degradation reactions at the Li metal surface for 1 M LiTFSI in DOL,[35−37] a typical electrolyte used in batteries.

To provide a training set of QM data to train the ReaxFF for LiTFSI, we use the B3LYP[38] hybrid flavor of density functional method with the 6-311+G(d,p) basis set. All QM calculations were conducted using Jaguar 8.8. During the HAIR simulations, the forces and dynamics for the AIMD lithium-electrolyte model were calculated using the Vienna ab Initio Simulation Package (VASP 5.4.4), while the ReaxFF simulations used the Large-scale Atomic/Molecular Massively Parallel Simulator (LAMMPS 2018) software.

The AIMD simulation used the Perdew−Burke−Ernzerhof (PBE) functional to describe the electron exchange and correction energies within the generalized gradient approximation (GGA). To describe the London dispersion integrations, we added the Grimme D3 correction. The projector augmented wave (PAW) method as implemented in VASP was utilized. A $1 \times 1 \times 1$ Monkhorst−Pack k-point mesh was used to sample the Brillouin zone integration, and we chose a 400 eV energy cutoff for plane-wave basis expansion. We used a Gaussian smearing width of 0.2 eV. The threshold for the electronic structure convergence of the self-consistent field was set to 10^{-4} eV.

In the HAIR procedure, the AIMD and ReaxFF MD simulations are conducted alternatively using the NVT ensemble at 300 K, which fixes the molecule numbers (N), volume (V), and temperature (T). Moreover, the time steps for AIMD and ReaxFF were set at 1 and 0.25 fs, respectively, to guarantee good energy conservation during the HAIR simulations while ensuring efficient convergence for collisions and smooth reactions. All HAIR simulations were conducted for 120 cycles (660 ps). In this work, we focus on the liquid electrolyte, in which diffusion is fast. So we consider a 10-time acceleration to be sufficient. Our future work will move forward to a solid electrolyte, for which a 10-time acceleration is likely not enough, perhaps requiring 100 times.

For the purpose of describing the lithium electrolyte system accurately, the ReaxFF parameters were extended to describe Li-TFSI. In the training set, we bond a hydrogen atom to the TFSI radical to obtain a neutral molecule. Table 1 exhibits the main decomposition reaction energies from QM and ReaxFF simulations. The gas-phase bond dissociation energies for C−F, C−S, and N−S bond cleavages are 104.4, 53.1, and 49.8 kcal/mol with ReaxFF, which are similar and in the same order as the QM values, 114.9, 50.3, and 50.2 kcal/mol, respectively. This indicates that C−S and N−S bond breaking are the most plausible initial decomposition pathways, not C−F bond breaking. This result that the Li salt initiates breaks the C−S or N−S bonds is in good agreement with the results of previous work.[37] Furthermore, the mean absolute deviations (MAD) between the QM results and ReaxFF predictions are 0.045 Å for

https://dx.doi.org/10.1021/acs.jpclett.0c03720
J. Phys. Chem. Lett. 2021, 12, 1300−1306

Table 1. Relative Reaction Energies (in kcal/mol) for QM and ReaxFF Calculations

reaction	relative reaction energies (kcal/mol) QM(B3LYP/6-311+g(d,p))	ReaxFF
$HN(SO_2CF_3)_2$=$HN(SO_2CF_3)SO_2CF_2$+F	114.9	104.4
$HN(SO_2CF_3)_2$=$HN(SO_2CF_3)SO_2$+CF_3	50.3	53.1
$HN(SO_2CF_3)_2$=$HNSO_2CF_3$+SO_2CF_3	50.2	49.8

bond distances and 3° for bond angles (Figure 1). More details about the fitting force field parameters and bond dissociation curves are in the Supporting Information.

Reactive dynamics simulations were conducted using the HAIR method with the NVT canonical ensemble at T = 300 K. Figure 2a,b shows the temperatures (T) for AIMD and ReaxFF during HAIR simulations. This shows a smooth transition between the AIMD and ReaxFF periods, suggesting continuous and smooth molecular dynamics simulations.

In order to explore the initial mechanism for a degradative reduction of the lithium electrolyte system, we monitored MD trajectories during HAIR simulations. As exhibited in Figure 3, the degradation reaction initiates by breaking the N−S bond of TFSI, forming two fragments at ∼6.0 ps. This decomposition process is consistent with previous theoretical and experimental results.[23,39,40] During the 6.0−11.0 ps period, the SO_2CF_3 fragment was reduced by Li^0 to form LiF, which has been regarded as an important component of the SEI layer investigated by the experimental method.[41,42]

Furthermore, lithium induced the ring of the DOL electrolyte to open, forming $CH_2OCH_2CH_2O$, as observed by Camacho-Forero[43] using AIMD. In the following segment (11.0−22.5 ps), the oxygen and fluorine atoms broke away from the fragment SO_2CF_3 step by step to form the stable products Li_2O and LiF. In Figure 4, the NSO_2CF_3 fragment decomposes into CF_3 and NSO_2 via C−S bond cleavage at 27.6 ps, just as in the QM trajectory, which was predicted to be the possible reaction pathway.[44] Subsequently, the decomposition fragments CF_3 and NSO_2 also undergo reduction reactions from Li_2O and LiF. Moreover, we also observed C_2H_4 and CH_2O at 33.0 ps, from $CH_2OCH_2CH_2O$ degradative reduction via a C−O bond breaking.

Camacho-Forero[43] proposed this decomposition reaction mechanism for DOL and calculated the reaction pathway of the DOL decomposition. In addition, Zhang[37] investigated the detailed PES pathway of DOL decomposition using QM calculations, finding that DOL experienced a ring-opening process followed by a conversion into C_2H_4 and CH_2O_2 fragments. The C_2H_4 has been mentioned as an important product during the reduction of electrolyte DOL. Additionally, similar ring-opening and C_2H_4 emission mechanisms have been reported by Yun[45] using the ReaxFF method to clarify the EC decomposition reaction mechanism. It has been demonstrated that the decomposition of DOL can be either accelerated by an extra charge[43] or Li atom.[36] Thus, these experimental and theoretical results not only indicate the reliability of the reduction reaction mechanism explored using the HAIR method but also prove that the HAIR scheme can accelerate the mass transfer of Li.

The detailed MD simulation trajectories were monitored, and the reaction mechanism was clarified within 49.5 ps as illustrated in Figure 5. The decomposition reaction for TFSI was initiated by N−S bond breaking to form NSO_2CF_3 and SO_2CF_3 fragments. The initial reactions of the Li salts are supported by QM calculations and by high-accuracy AIMD simulations and experimental results. Subsequently, these fragments undergo multiple reduction reactions along with the removal of fluorine or oxygen atoms. The main products, including Li_2O and LiF, were verified as the components of the SEI layer according to previous experimental results.[16] In the degradation reactions of the DOL electrolyte, both ring-opening and C_2H_4 elimination processes were observed during the reaction-diffusion (RD) simulations, which are consistent with both QM calculations and experimental observations. Therefore, the proposed HAIR method retains the accuracy of AIMD simulations with a low computational cost; the simulation results were supported by experimental observations.[37,45]

Figure 6a−c exhibits the radial distribution function from the HAIR MD simulations at 22 and 660 ps. A sharp peak arises at 2 Å for Li−F and Li−O, indicating additional products (LiF and Li_2O) produced at 660 ps. The snapshots from RD simulations in Figure 6d,e, show significant differences that clarify the main products or fragments at 22 and 660 ps. As shown in Table 2, the

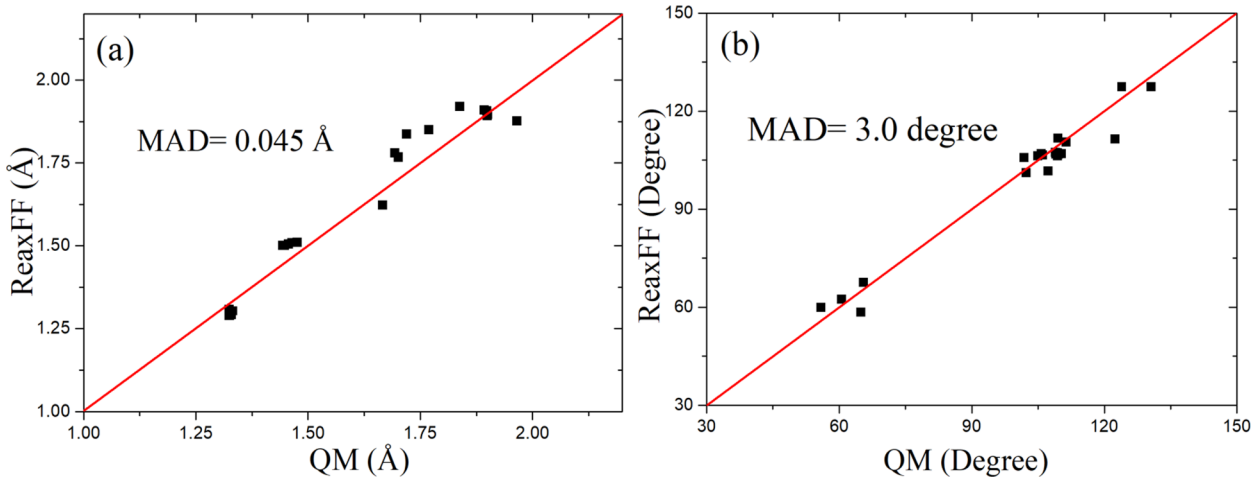

Figure 1. Comparison of training set geometries predicted by QM and ReaxFF methods. (a) Bond distances. (b) Bond angles.

https://dx.doi.org/10.1021/acs.jpclett.0c03720
J. Phys. Chem. Lett. 2021, 12, 1300−1306

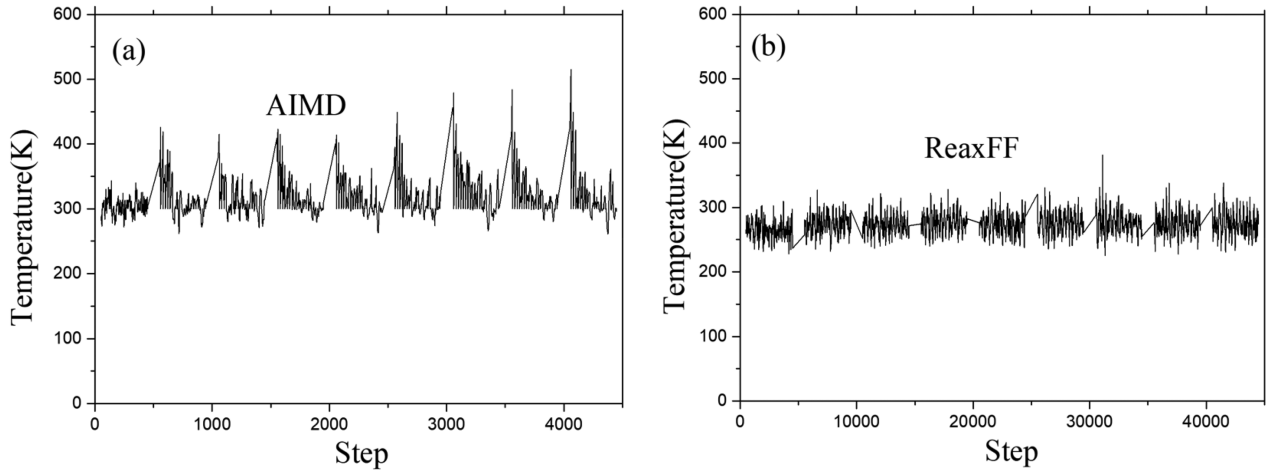

Figure 2. Temperatures for (a) AIMD and (b) ReaxFF during HAIR simulations.

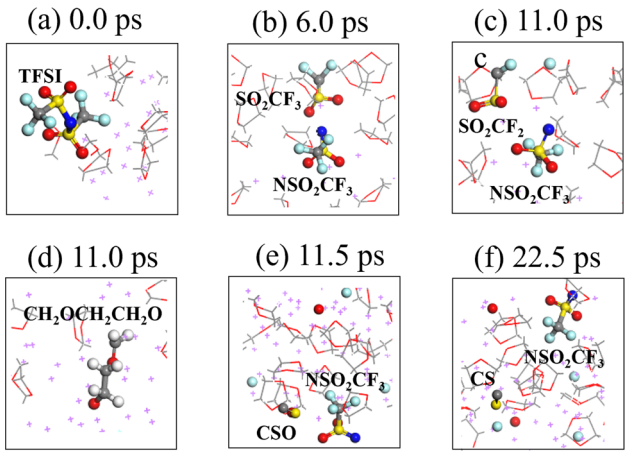

Figure 3. Sequence of TFSI and DOL decompositions obtained from HAIR simulations for the DOL/LiTFSI mixture between 0 and 22.5 ps. (a) 0.0, (b) 6.0, (c) 11.0, (d) 11.0, (e) 11.5, and (f) 22.5 ps. Color code: lithium, purple; oxygen, red; carbon, gray; fluorine, cyan; sulfur, yellow, nitrogen, blue; hydrogen, white.

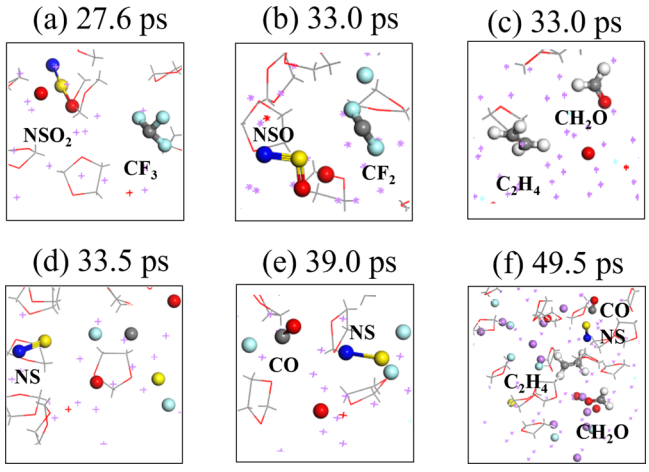

Figure 4. Sequence of NSO_2CF_3 and DOL decomposition obtained from HAIR simulations for DOL/LiTFSI mixture between 27.6 and 49.5 ps. (a) 27.6, (b) 33.0, (c) 33.0, (d) 33.5, (e) 39.0, and (f) 49.5 ps. Color code as in Figure 3.

products and fragments at 22 ps form mainly by direct decomposition of TFSI, leading to Li_2O, LiF, NSO_2CF_3, CSO, and a ring-opened molecule of DOL (by Li^0) to form $CH_2OCH_2CH_2OLi$. With regard to 660 ps, further reactions are observed with stable products, including C_2H_4, CH_2O, LiF, Li_2O, etc. Recently, Ospina-Acevedo et al. carried out ReaxFF MD simulations up to 20 ns to simulate the initial nucleation of SEI for electrolytes include $LiPF_6$ and $LiCF_3SO_3$ in DME, DOL, fluoroethylene carbonate (FEC), and ethylene carbonate (EC).[26] In our HAIR simulation, stable clusters consisting of Li^+ and various anions (such as Ox^- and F^-) have already appeared in the 660 ps simulation (Figure S5a), which has no substantial difference when compared with that in the 20 ns simulation (Figure S5b). The difference between our work and that of Ospina-Acevedo should be from the different simulation systems and protocols.

In summary, we introduce here a new Hybrid AIMD-ReaxFF scheme (HAIR) that combines QM and MM reactive dynamics, and we apply it to investigate the degradation reduction reactions of the lithium electrolyte system. The HAIR simulation is implemented by alternating between AIMD and ReaxFF RD with a smooth connection. To conduct the ReaxFF procedure, ReaxFF parameters for LiTFSI were optimized using the MC force field optimization method. We found that the predictions of the ReaxFF method exhibit good agreement with the QM results, which implies suitable descriptions for a Li salt containing system.

To explore the reaction mechanism of the degradation of the electrolyte on the lithium electrode, we performed RD simulations using the HAIR method for 660 ps. Our RD simulation trajectories show that TFSI decomposition is initiated by a N−S bond cleavage to form NSO_2CF_3 and SO_2CF_3. Subsequently, fluorine and oxygen atoms break off from NSO_2CF_3 and SO_2CF_3 step by step to form the stable products Li_2O and LiF.

For the DOL electrolyte, we observed ring-opening and C_2H_4 emission processes similar to the predictions by Yun.[45] Our RD using the HAIR method are in accordance with QM and experimental results. But the computational efficiency of the HAIR method increases the total time covered by a factor of 10−660 ps, far too long for AIMD but with the same accuracy as AIMD simulations.

https://dx.doi.org/10.1021/acs.jpclett.0c03720
J. Phys. Chem. Lett. 2021, 12, 1300−1306

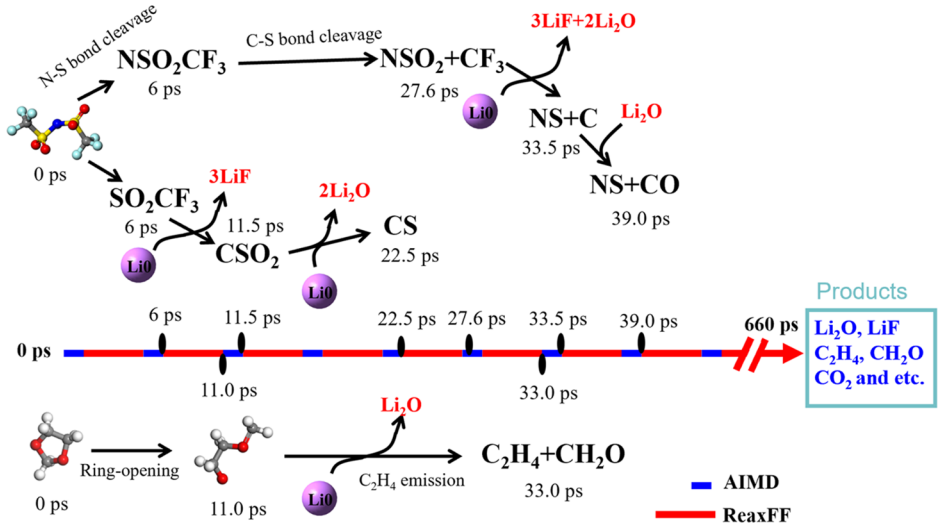

Figure 5. Reaction pathway obtained from HAIR simulations for LiTFSI and DOL.

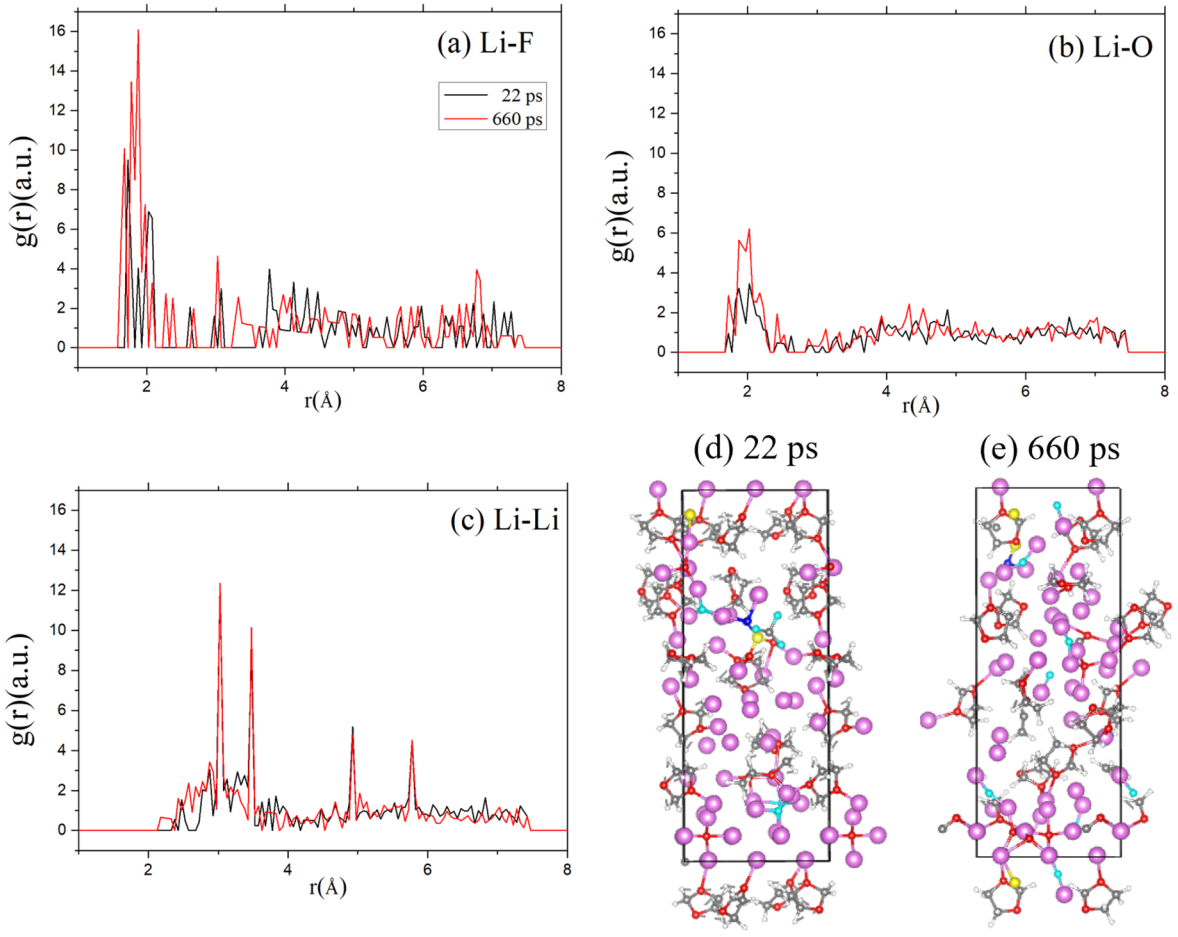

Figure 6. Radial distribution function for (a) Li−F, (b) Li−O, and (c) Li−Li and snapshots from an MD simulation at (d) 20 and (e) 660 ps.

Table 2. Products Obtained from HAIR MD Simulation at 22 and 660 ps

simulation time	products or fragments
20 ps	Li_2O, LiF, NSO_2CF_3, CSO, $CH_2OCH_2CH_2OLi$
660 ps	C_2H_4, CH_2O, LiF, Li_2O, CO, CO_2, CS, NS, LiH, C_2H_3Li

■ ASSOCIATED CONTENT

Supporting Information

The Supporting Information is available free of charge at https://pubs.acs.org/doi/10.1021/acs.jpclett.0c03720.

Details of the Hybrid AIMD-ReaxFF scheme, reactive force-field parameters optimization and force-field parameters, model of the lithium-electrolyte system,

https://dx.doi.org/10.1021/acs.jpclett.0c03720
J. Phys. Chem. Lett. 2021, 12, 1300−1306

XRD patterns from MD simulations at 22 and 660 ps, and results of 20 ns simulation (PDF)

General parameters (TXT)

Computer algorithm (TXT)

AUTHOR INFORMATION

Corresponding Authors

Tao Cheng − *Institute of Functional Nano and Soft Materials, Soochow University, Suzhou 215123, China;* orcid.org/0000-0003-4830-177X; Email: tcheng@suda.edu.cn

William A Goddard, III − *Materials and Process Simulation Center, Pasadena 91125, California, United States;* orcid.org/0000-0003-0097-5716; Email: wag@caltech.edu

Authors

Yue Liu − *Institute of Functional Nano and Soft Materials, Soochow University, Suzhou 215123, China*

Peiping Yu − *Institute of Functional Nano and Soft Materials, Soochow University, Suzhou 215123, China*

Yu Wu − *Institute of Functional Nano and Soft Materials, Soochow University, Suzhou 215123, China*

Hao Yang − *Institute of Functional Nano and Soft Materials, Soochow University, Suzhou 215123, China;* orcid.org/0000-0002-8241-6231

Miao Xie − *Institute of Functional Nano and Soft Materials, Soochow University, Suzhou 215123, China;* orcid.org/0000-0002-9797-1449

Liyuan Huai − *Institute of New Energy Technology, Ningbo Institute of Materials Technology & Engineering, Chinese Academy of Sciences, Ningbo 315201, China*

Complete contact information is available at: https://pubs.acs.org/10.1021/acs.jpclett.0c03720

Notes

The authors declare no competing financial interest.

ACKNOWLEDGMENTS

T.C. and M.X. thank the National Natural Science Foundation of China (21903058 and 22003044), the Natural Science Foundation of Jiangsu Higher Education Institutions (SBK20190810), the Jiangsu Province High-Level Talents (JNHB-106), and the Priority Academic Program Development of Jiangsu Higher Education Institutions for financial support. H.Y. thanks China Postdoctoral Science Foundation (2019M660128) for financial support. This work was partly supported by the Collaborative Innovation Center of Suzhou Nano Science & Technology. W.A.G. received support from the United States National Science Foundation (CBET-1805022 and CBET-2005250)

REFERENCES

(1) Bilgen, S. Structure and Environmental Impact of Global Energy Consumption. *Renewable Sustainable Energy Rev.* **2014**, *38*, 890−902.

(2) Tarascon, J. M.; Armand, M. Issues and Challenges Facing Rechargeable Lithium Batteries. *Nature* **2001**, *414*, 359−367.

(3) Dunn, B.; Kamath, H.; Tarascon, J.-M. Electrical Energy Storage for the Grid: A Battery of Choices. *Science* **2011**, *334*, 928−935.

(4) Goodenough, J. B.; Park, K. S. The Li-Ion Rechargeable Battery: A Perspective. *J. Am. Chem. Soc.* **2013**, *135*, 1167−1176.

(5) Lin, D.; Liu, Y.; Cui, Y. Reviving the Lithium Metal Anode for High-Energy Batteries. *Nat. Nanotechnol.* **2017**, *12*, 194−206.

(6) Bruce, P. G.; Freunberger, S. A.; Hardwick, L. J.; Tarascon, J. M. Li-O_2 and Li-S Batteries with High Energy Storage. *Nat. Mater.* **2012**, *11*, 19−29.

(7) Huang, C.; Xiao, J.; Shao, Y.; Zheng, J.; Bennett, W. D.; Lu, D.; Saraf, L. V.; Engelhard, M.; Ji, L.; Zhang, J.; et al. Manipulating Surface Reactions in Lithium-Sulphur Batteries Using Hybrid Anode Structures. *Nat. Commun.* **2014**, *5*, 3015.

(8) Shi, F.; Pei, A.; Boyle, D. T.; Xie, J.; Yu, X.; Zhang, X.; Cui, Y. Lithium Metal Stripping Beneath the Solid Electrolyte Interphase. *Proc. Natl. Acad. Sci. U. S. A.* **2018**, *115*, 8529−8534.

(9) Scheers, J.; Fantini, S.; Johansson, P. A Review of Electrolytes for Lithium−Sulphur Batteries. *J. Power Sources* **2014**, *255*, 204−218.

(10) Barghamadi, M.; Kapoor, A.; Wen, C. A Review on Li-S Batteries as a High Efficiency Rechargeable Lithium Battery. *J. Electrochem. Soc.* **2013**, *160*, A1256−A1263.

(11) Dey, A. N. Film Formation on Lithium Anode in Propylene Carbonate. *J. Electrochem. Soc.* **1970**, *117*, C248.

(12) Peled, E.; Golodnitsky, D.; Ardel, G. Advanced Model for Solid Electrolyte Interphase Electrodes in Liquid and Polymer Electrolytes. *J. Electrochem. Soc.* **1997**, *144*, L208−L210.

(13) Aurbach, D.; et al. New Insights into the Interactions between Electrode Materials and Electrolyte Solutions for Advanced Non-aqueous Batteries. *J. Power Sources* **1999**, *81*, 95−111.

(14) Verma, P.; Maire, P.; Novak, P. A Review of the Features and Analyses of the Solid Electrolyte Interphase in Li-ion Batteries. *Electrochim. Acta* **2010**, *55*, 6332−6341.

(15) Nazri, G.; Muller, R. H. Composition of Surface Layers on Li Electrodes in PC, $LiClO_4$ of Very Low Water Content. *J. Electrochem. Soc.* **1985**, *132*, 2050−2054.

(16) Xu, K. Electrolytes and Interphases in Li-Ion Batteries and Beyond. *Chem. Rev.* **2014**, *114*, 11503−11618.

(17) Agubra, V. A.; Fergus, J. W. The Formation and Stability of the Solid Electrolyte Interface on the Graphite Anode. *J. Power Sources* **2014**, *268*, 153−162.

(18) Ramos-Sanchez, G.; et al. Computational Studies of Interfacial Reactions at Anode Materials: Initial Stages of the Solid-Electrolyte-Interphase Layer Formation. *J. Electrochem. En. Conv. Stor.* **2016**, *13*, 031002.

(19) Aurbach, D.; Daroux, M. L.; Faguy, P. W.; Yeager, E. Identification of Surface Films Formed on Lithium in Propylene Carbonate Solutions. *J. Electrochem. Soc.* **1987**, *134*, 1611−1620.

(20) Wang, Y.; Liu, Y.; Tu, Y.; Wang, Q. Reductive Decomposition of Solvents and Additives toward Solid Electrolyte Interphase Formation in Lithium-Ion Battery. *J. Phys. Chem. C* **2020**, *124*, 9099−9108.

(21) Wang, A.; Kadam, S.; Li, L.; Shi, S.; Qi, Y. Review on Modeling of the Anode Solid Electrolyte Interphase (SEI) for Lithium-Ion Batteries. *npj Computational Materials* **2018**, *4*, 15.

(22) Camacho-Forero, L. E.; Smith, T. W.; Bertolini, S.; Balbuena, P. B. Reactivity at the Lithium−Metal Anode Surface of Lithium−Sulfur Batteries. *J. Phys. Chem. C* **2015**, *119*, 26828−26839.

(23) Kamphaus, E. P.; Angarita-Gomez, S.; Qin, X.; Shao, M.; Engelhard, M.; Mueller, K. T.; Murugesan, V.; Balbuena, P. B. Role of Inorganic Surface Layer on Solid Electrolyte Interphase Evolution at Li-Metal Anodes. *ACS Appl. Mater. Interfaces* **2019**, *11*, 31467−31476.

(24) Bertolini, S.; Balbuena, P. B. Buildup of the Solid Electrolyte Interphase on Lithium-Metal Anodes: Reactive Molecular Dynamics Study. *J. Phys. Chem. C* **2018**, *122*, 10783−10791.

(25) Camacho-Forero, L. E.; Smith, T. W.; Balbuena, P. B. Effects of High and Low Salt Concentration in Electrolytes at Lithium−Metal Anode Surfaces. *J. Phys. Chem. C* **2017**, *121*, 182−194.

(26) Ospina-Acevedo, F.; Guo, N.; Balbuena, P. B. Lithium Oxidation and Electrolyte Decomposition at Li-Metal/Liquid Electrolyte Interfaces. *J. Mater. Chem. A* **2020**, *8*, 17036−17055.

(27) van Duin, A. C. T.; Dasgupta, S.; Lorant, F.; Goddard, W. A. ReaxFF: A Reactive Force Field for Hydrocarbons. *J. Phys. Chem. A* **2001**, *105*, 9396−9409.

(28) Chenoweth, K.; van Duin, A. C. T.; Goddard, W. A. ReaxFF Reactive Force Field for Molecular Dynamics Simulations of Hydrocarbon Oxidation. *J. Phys. Chem. A* **2008**, *112*, 1040−1053.

(29) Bedrov, D.; Smith, G. D.; van Duin, A. C. T. Reactions of Singly-Reduced Ethylene Carbonate in Lithium Battery Electrolytes: A Molecular Dynamics Simulation Study Using the ReaxFF. *J. Phys. Chem. A* **2012**, *116*, 2978−2985.
(30) Islam, M. M.; Kolesov, G.; Verstraelen, T.; Kaxiras, E.; van Duin, A. C. T. eReaxFF: A Pseudoclassical Treatment of Explicit Electrons within Reactive Force Field Simulations. *J. Chem. Theory Comput.* **2016**, *12*, 3463−3472.
(31) O'Hearn, K. A.; Swift, M. W.; Liu, J.; Magoulas, I.; Piecuch, P.; van Duin, A. C. T.; Aktulga, H. M.; Qi, Y. Optimization of the Reax Force Field for the Lithium−Oxygen System Using a High Fidelity Charge Model. *J. Chem. Phys.* **2020**, *153*, 084107.
(32) Islam, M. M.; Bryantsev, S. V.; van Duin, A. C. T. ReaxFF Reactive Force Field Simulations on the Influence of Teflon on Electrolyte Decomposition During Li/SWCNT Anode Discharge in Lithium-Sulfur Batteries. *J. Electrochem. Soc.* **2014**, *161* (8), E3009−E3014.
(33) Metropolis, N.; Rosenbluth, A. W.; Rosenbluth, M. N.; Teller, A. H.; Teller, E. Equation of State Calculations by Fast Computing Machines. *J. Chem. Phys.* **1953**, *21*, 1087−1092.
(34) Kirkpatrick, S.; Gelatt, C. D.; Vecchi, M. P. Optimization by Simulated Annealing. *Science* **1983**, *220*, 671.
(35) Mikhaylik, Y. V.; Akridge, J. R. Low Temperature Performance of Li/S Batteries. *J. Electrochem. Soc.* **2003**, *150* (3), A306−A311.
(36) Agostini, M.; Scrosati, B.; Hassoun, J. An Advanced Lithium-Ion Sulfur Battery for High Energy Storage. *Adv. Energy Mater.* **2015**, *5* (16), 1500481.
(37) Chen, X.; Hou, T. Z.; Li, B.; Yan, C.; Zhu, L.; Guan, C.; Cheng, X. B.; Peng, H. J.; Huang, J. Q.; Zhang, Q. Towards Stable Lithium-Sulfur Batteries: Mechanistic Insights into Electrolyte Decomposition on Lithium Metal Anode. *Energy Storage Mater.* **2017**, *8*, 194−201.
(38) Becke, A. D. Density-Functional Thermochemistry. III. The Role of Exact Exchange. *J. Chem. Phys.* **1993**, *98*, 5648−5652.
(39) Sodeyama, K.; Yamada, Y.; Aikawa, K.; Yamada, A.; Tateyama, Y. Sacrificial Anion Reduction Mechanism for Electrochemical Stability Improvement in Highly Concentrated Li-Salt Electrolyte. *J. Phys. Chem. C* **2014**, *118*, 14091−14097.
(40) Merinov, B. V.; Zybin, S. V.; Naserifar, S.; Morozov, S.; Oppenheim, J.; Goddard, W. A.; Lee, J.; Lee, J. H.; Han, H. E.; Choi, Y. C.; et al. Interface Structure in Li-Metal/$[Pyr_{14}][TFSI]$-Ionic Liquid System from *ab initio* Molecular Dynamics Simulations. *J. Phys. Chem. Lett.* **2019**, *10*, 4577−4586.
(41) Li, N.-W.; Yin, Y.-X.; Yang, C.-P.; Guo, Y.-G. An Artificial Solid Electrolyte Interphase Layer for Stable Lithium Metal Anodes. *Adv. Mater.* **2016**, *28*, 1853−1858.
(42) Menkin, S.; Golodnitsky, D.; Peled, E. Artificial Solid-Electrolyte Interphase (SEI) for Improved Cycleability and Safety of Lithium−Ion Cells for EV Applications. *Electrochem. Commun.* **2009**, *11*, 1789−1791.
(43) Camacho-Forero, L. E.; Balbuena, P. B. Effects of Charged Interfaces on Electrolyte Decomposition at the Lithium Metal Anode. *J. Power Sources* **2020**, *472*, 228449.
(44) Haskins, J. B.; Yildirim, H.; Bauschlicher, C. W., Jr.; Lawson, J. W. Decomposition of Ionic Liquids at Lithium Interfaces. 2. Gas Phase Computations. *J. Phys. Chem. C* **2017**, *121*, 28235−28248.
(45) Yun, K.-S.; Pai, S. J.; Yeo, B. C.; Lee, K.-R.; Kim, S.-J.; Han, S. S. Simulation Protocol for Prediction of a Solid-Electrolyte Interphase on the Silicon-Based Anodes of a Lithium-Ion Battery: ReaxFF Reactive Force Field. *J. Phys. Chem. Lett.* **2017**, *8*, 2812−2818.

https://dx.doi.org/10.1021/acs.jpclett.0c03720
J. Phys. Chem. Lett. 2021, 12, 1300−1306